Modeling the Influence of Hydrodynamic Processes on Anchovy Distribution and Connectivity in the Black Sea

Bettina A. Fach[1],*

[1] Middle East Technical University, Institute of Marine Sciences, PO Box 28, 33731, Erdemli, Turkey.

Abstract

Dispersal mechanisms of Black Sea anchovy larvae (*Engraulis encrasicolus ponticus*) across the Black Sea were studied with an individual based anchovy larvae model embedded in a Lagrangian model using surface currents calculated from daily dynamic height topography maps of altimeter data during a period of three years (2001-2003). Particles representing anchovy eggs were released at different sites during June to August and their movement was tracked over time. Drifters were advected for 36 days, representing the time it generally takes for anchovy eggs to develop into juveniles. Each individual was subject to somatic growth whose temperature dependence was calculated from satellite derived sea surface temperature data.

Model results indicate that larval dispersal in the Black Sea is strongly controlled at the basin scale by the Rim Current circulation and its two cyclonic basin-wide gyres. It is locally controlled by mesoscale eddies. Consistent with the observed circulation fields, a strong meridional transport exists from the northern to the southern coastal zone along the western coast and the central basin. The peripheries of both the western and the eastern cyclonic gyres are also associated with strong larval transport from the southern coast to offshore areas. Elsewhere the connectivity between different regions is not as well pronounced due to weaker and patchy current fields. Variability in the dispersal of larvae is considerable when comparing different years and seasons and should be taken into account when designing networks of Marine Protected Areas in the Black Sea.

Keywords: Black Sea anchovy larvae, Black Sea circulation, connectivity, Lagrangian modeling, temperature dependence.

Karadeniz'deki Hamsi Dağılımı ve Bölgeler Arası Bağlantısı üzerine Hidrodinamik Proseslerin Etkisinin Modellenmesi

Özet

Karadeniz hamsi larvalarının (*Engraulis encrasicolus ponticus*) Karadeniz baseninde dağılım mekanizmaları, geliştirilen bir birey tabanlı hamsi larva modelinin üç yıllık (2001-2003) altimetre verisinden hesaplanmış yüzey akıntıları kullanılarak bir Lagrangian modeline entegrasyonu ile araştırılmıştır. Model içinde hamsi yumurtalarını temsil eden parçacıklar Haziran-Ağustos ayları arasında farklı noktalarda bırakılmış ve zamana bağlı hareketleri takip edilmiştir. Hamsi yumurtalarının juvenil bireye gelişim süresi (ortalama) olan 36 gün boyunca model içinde bu parçacıklar akıntıya bağlı hareket etmiştir. Daha sonra bu bireylerin uydu verisinden hesaplanan yüzey suyu sıcaklık verisine bağlı olarak somatik büyümeleri hesaplanmıştır.

Model sonuçları göstermiştir ki Karadeniz'de basen ölçeğinde larval dağılımı kontrol eden en büyük faktör kıyı akıntısı (Rim Current) ve iki büyük ölçekli siklonik döngüdür. Yerel ölçekte ise orta ölçek (mesoscale) girdaplar önem kazanır. Gözlemlenen akıntı sistemleri ile de tutarlı olarak, orta ve batı basende kuzey kıyılarından güneye güçlü bir boylamsal taşınım oluşur. Model sonuçları ayrıca batı ve doğu siklonik döngülerinin çevrelerinde güney sahillerinden güçlü larval taşınım olduğunu önermektedir. Geri kalan bölgelerde ise zayıf ve dağınık akıntılardan dolayı bölgeler arası bağlantı görülmemektedir. Farklı yıllar ve mevsimler karşılaştırıldığında larvaların dağılımında ortaya ciddi farklılıklar çıkmaktadır ki buda Karadeniz'de özellikle koruma bölgeleri tasarlanırken göz önüne alınması gereken bir etkendir.

Anahtar Kelimeler: Karadeniz, hamsi larvası, akıntı, bölgeler arası bağlantı, Lagrangian modelleme, sıcaklığa bağlı değişim.

Introduction

Importance of Dispersal During Early Life

In many marine populations, dispersal occurs during early life through advection by ocean currents, when young individuals are not yet capable of active movement. Older life stages exhibit behavior and active movement and can therefore often move on different spatial scales. Advection by large-scale

circulation has a strong influence on the direction and extent of dispersal in early life stages that then influences population success and persistence. Identifying the scale of such exchange (connectivity) among marine populations, as well as determining the factors that may drive this exchange is of importance for understanding population dynamics and still remains a challenge today (Cowen *et al.*, 2006). Many marine fisheries today target fish stocks that are structured by their physical environment and therefore the spatial relationships between physical and biological processes are of great importance when attempting to understand their population dynamics, distribution and abundance.

Larval dispersal by ocean currents and connectivity between different oceanic regions have been identified as crucial factors for structuring marine populations (Cowen *et al.*, 2006) as well as for designing networks of Marine Protected Areas (MPAs) (Moffit *et al.*, 2009; Lester *et al.*, 2009). While marine population connectivity depends on a multitude of factors such as habitat availability, spawning efficiency, larval dispersal, trophic interactions and adult movements (Cowen and Sponaugle, 2009; Game *et al.*, 2009), larval dispersal has been identified as a crucial factor for structuring oceanic populations (Cowen *et al.*, 2006), for determining broad-scale ecological connectivity (Treml *et al.*, 2012), and for playing a major role in assuring population persistence in a MPA network (Moffitt *et al.*, 2011). Therefore, patterns and magnitude of larval connectivity have been used as a tool to design MPAs (Lester *et al.*, 2009) and also assess their efficiency (Pelc *et al.*, 2010).

To understand the level of dispersal and hence connectivity between different areas, tagging of animals is often not possible because of the small size of the individuals in their early life stages, and the large numbers of tagged animals needed to be able to recapture enough of them. An alternative approach is to test connectivity using particle simulations (Cowen *et al.*, 2006, Fach and Klinck, 2006; Ashford *et al.*, 2010). In this study, such tracking of the large-scale physical transport pathways in the Black Sea together with a simple, temperature dependent anchovy larvae growth model was applied to assess the dispersal of pelagic anchovy larvae.

Black Sea Circulation

The Black Sea is a nearly enclosed basin connected to the Sea of Marmara and the Sea of Azov by the narrow Bosporus and Kerch Straits, respectively. The only major shelf region of the Black Sea is the northwestern shelf where the three largest rivers of the Black Sea, the Danube, Dniepr and Dniestr, discharge. The general circulation of the Black Sea is driven by this large freshwater input on the northwestern shelf as well as wind stress and is steered by the steep topography around its periphery that consists of narrow shelves and a maximum depth of around 2200 m (Oguz *et al.*, 2005). The circulation is composed of a meandering, cyclonic Rim current and two cyclonic cells within the interior basin (Figure 1). This general circulation is known to have a seasonal cycle, with its characteristic features repeating every year with some year-to-year variability (Korotaev *et al.*, 2003). In addition, the mesoscale circulation is characterized by a number of anticyclonic eddies forming on the coastal side of the Rim Current: Bosphorus, Batumi, Sukhumi, Caucasus, Kerch, Crimea, Sevastopol, Danube, Constantsa, and Kaliakra eddies (Figure 1). Current speeds in the upper layer of the Rim current are 50-150 cm/s (Oguz and Besiktepe, 1999) and meanders of the Rim Current have a typical time scale of
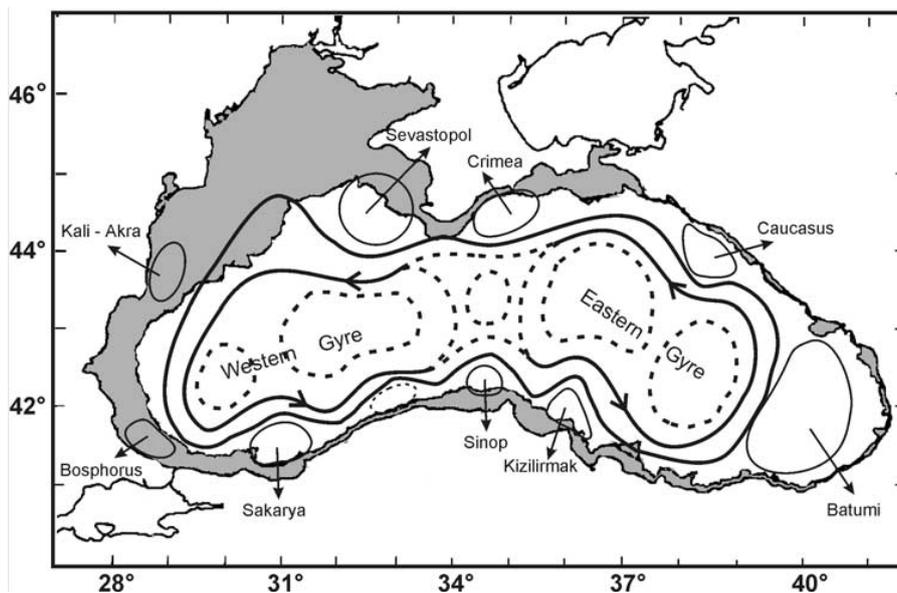
Figure 1. Schematic of the Black Sea general surface circulation (reproduced from Korotaev *et al.*, 2003). Names of quasi-permanent anticyclonic eddies are indicated with arrows on land near by.

persistence on the order of 50-150 days (Korataev *et al.*, 2003). Highly dynamic events such as meander steepening and propagation, ring formation and detachment take place on weekly time-scales and can lead to considerable exchange and transport between the coastal and offshore waters as has been shown with satellite chlorophyll data (Oguz *et al.*, 2002). Therefore they may constitute an important component of the Black Sea dynamics that is likely to influence the spatial distribution of anchovy eggs and larvae.

Black Sea Anchovy Early Life History

Black Sea anchovy has a high fecundity and long spawning season that lasts from May to September (Lisovenko and Andrianov, 1996). Spawning occurs most efficiently from June to August in water temperatures higher than 20°C, with optimal temperatures between 23-25°C (Niermann *et al.*, 1994; Lisovenko and Adrianov, 1996; Sorokin, 2002). Growth of Black Sea anchovy is characterized by its strong temperature dependence for the early-life stages (Lisovenko and Andrianov, 1996; Garcia and Palomera, 1996; North and Houde, 2004). Observations show that the pre-larval period (hatching and yolk-sac larva stages) of anchovy lasts for 2-2.5 days at water temperatures above 20°C (Lisovenko and Andrianov, 1996). The early larva phase (up to ~ 1.0 cm length) spans 12 days under typical conditions, the late larva phase (up to ~ 2.5 cm) 22 days and the juvenile stage about 32 days (Sorokin, 2002). Juveniles become Young of Year at about 4 cm and then reach sexual maturity at 6 cm (Lisovenkov and Andrianov, 1996). Juvenile anchovy are assumed to be able to start swimming after urostyle flexion.

Black Sea anchovy is described by Ivanov and Beverton (1985) and Chashchin (1996) to be spawning mainly in the northern Black Sea, specifically the northwestern shelf and the Crimea region, and then migrating to the south to overwinter in warm waters off the Turkish coast. In spring, the migration routes reverse and anchovy move north again for spawning purposes. However, studies focusing on the southern Black Sea have repeatedly shown anchovy spawning in the entire southern Black Sea (Einarsson and Gürtürk, 1960; Niermann *et al.*, 1994).

Models of anchovy larvae dispersal that include individual based models of different complexity have been applied to different regions such as the southern Benguela (Mullon *et al.*, 2003; Parada *et al.*, 2003), northern Aegean Sea (Politikos *et al.*, 2011), and the coast of Peru (Xu *et al.*, 2013) but not yet to the Black Sea. The use of such models gives insight into the early life cycle dispersal, the importance of different spawning grounds, as well as the influence of changing environmental conditions on the recruitment success of anchovy.

The aim of this research is to understand anchovy larval dispersal by currents in the Black Sea to be able to scale the connectivity of anchovy within the Black Sea and how such dispersal may influence larval survival through changing environmental conditions. This research is of importance for the design of MPA networks and ultimately, the interpretation of transport mechanisms will lead to a better understanding of the factors controlling anchovy distribution and production, which is needed for the management of this important commercially fished species.

Materials and Methods

Satellite Data

Black Sea surface velocity fields used for particle tracking were calculated from the Archiving, Validation and Interpretation of Satellite Oceanographic (AVISO) data Sea Level Anomalies (SLA) and geostrophic velocity anomalies regional product for the Black Sea. The altimeter products were produced by Ssalto/Duacs, the Ssalto (Segment Sol multimissions d'ALTimétrie, d'Orbitographie et de localisation précise) multimission altimeter data processing system) and distributed by AVISO, with support from Centre National d'Etudes Spatiales (CNES) http://www.aviso.oceanobs.com/en/data/products/sea-surface-height-products/regional/m-sla-black-sea/index.html. They are weekly, multi-mission sea surface heights anomalies gridded on a regular 1/8° x 1/8° grid. This weekly data was then interpolated to obtain daily sea surface height fields. The mean sea surface height provided by Korotaev *et al.* (2003) was then added to the daily AVISO fields to compute the geostrophic flow at the surface. Using only surface circulation fields in this study is a reasonable assumption for anchovy in the Black Sea, because eggs and larvae are found in the upper 10-20 m, above the seasonal thermocline, egg production not being possible in the Cold Intermediate Layer (~ 7°C) below the surface mixed layer (Niermann *et al.*, 1994; Kideys *et al.*, 1999; Satilmis *et al.*, 2003).

The temperature dependence of anchovy growth is estimated using the optimal interpolated Advanced Very High Resolution Radiometer (AVHRR) temperature product (http://gos.ifa.rm.cnr.it). The data were processed and made available by Gruppo di Oceanografia da Satellite (GOS) on a 1/16° x 1/16° grid. All satellite data used in this study were interpolated onto a 1/16° x 1/10° (7 km x 8 km) grid to ensure compatibility.

After analysis of satellite data of the past 2 decades three different years (2001 to 2003) which were very different in terms of temperature and surface circulation, were chosen for the simulations to assess the influence of environmental conditions on this dispersal. 2001 was chosen because it was an

anomalously warm year, compared to other years of the 1990s and 2000s, while 2003 was exceptionally cool in comparison (McQuatters-Gollop *et al*., 2008). Hence, three consecutive years represented a wide variety of environmental conditions in the Black Sea.

Lagrangian Particle Tracking

Pelagic larvae transport pathways were calculated from the surface circulation fields using a first-order accurate Lagrangian particle tracking scheme. The scheme calculates the position of each drifter in time (dx/dt) by integrating

$$\frac{d\tilde{x}}{dt} = \vec{u}(\vec{x}, t) , \qquad (1)$$

where the right-hand side is estimated through linear interpolation in time (*t*) and space (*x*) of daily surface velocity fields (*u*). The scheme was chosen because it is simple and computationally efficient and the choice of a very small time step (dt = 1 min) makes it comparable to a second-order accurate scheme ensuring appropriate accuracy. Sub-grid scale dispersion processes that cannot be resolved by discrete velocity fields are known to influence particle trajectories and are often included in particle tracking algorithms by superimposing a random walk term for each particle and time step (Cowen *et al*., 2006; Xue *et al*., 2008). This is omitted in this study because the satellite-based estimate of the surface circulation is already a rough approximation of the actual flow field that accounts for only the geostrophic part of the flow and artificially adding dispersion will not enhance simulation results.

For the purpose of this theoretical modeling study, anchovy eggs were assumed to be present in 11

coastal regions with depths less than 2000m (Figure 2, 1-11) that are generally accepted spawning areas throughout the Black Sea (Einarson and Gürtürk, 1960; Ivanov and Beverton, 1985; Niermann *et al*., 1994; Chashchin, 1996). Because observations show that anchovy eggs are found in open water areas of most of the Black Sea as well (Einarson and Gürtürk, 1960; Niermann *et al*., 1994), the open sea (>2000 m) was divided into another 4 areas (Figure 2, Area 12-15) to better identify the connectivity of spawning and overwintering grounds.

Using the Lagrangian tracking code, the trajectories of drifters released throughout the entire Black Sea (Figure 2) were tracked over time. A total of 7175 particles were released each time in mid-June (15th), mid-July and mid-August of three consecutive years (2001-2003) in areas where the water temperature was found to be above 20°C. Since this study is focused on estimating the influence of circulation patterns on the anchovy population distribution throughout the entire Black Sea, the model includes only the non-motile stages of anchovy (pre-larval, early larva and late larva phases) that are tracked for 36 days, the typical time period of anchovy development into juveniles (Dulcic, 1997). Since only the non-motile stages are considered, the anchovy larvae are assumed to be passive drifters without any active swimming and fishing mortality. These simplifications isolate the effect of environmental influences on anchovy connectivity and reduce complexity of this exploratory study.

Anchovy Larval IBM

Because temperature is a critical factor for anchovy early-life stages (Lisovenko and Andrianov, 1996; Garcia and Palomera, 1996; North and Houde,
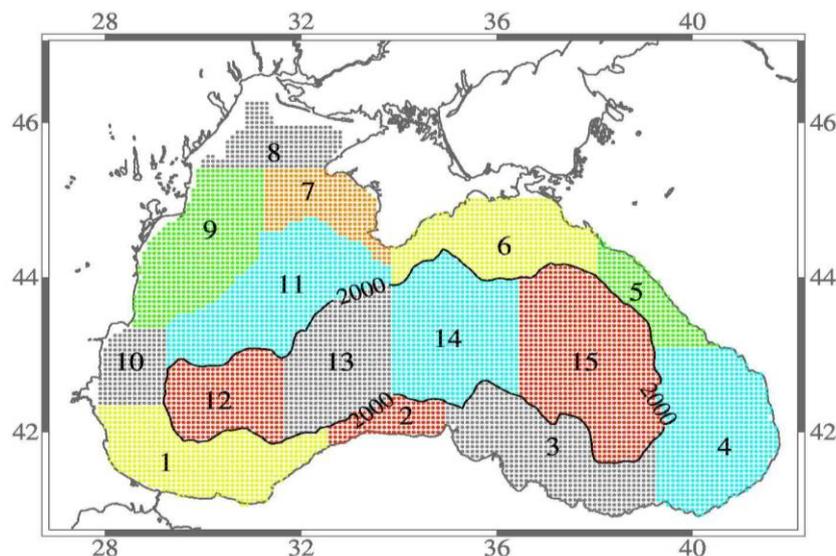
Figure 2. Release areas for model anchovy. Colored dots mark the release points belonging to each area. Thin black line marks the 2000m isobath.

2004) anchovy was assumed to grow and develop based on a simple temperature dependence. In the model, anchovy development is divided into 5 different phases: eggs, yolk-sac larva, early larva (<10 mm), larva (<20 mm) and late larva. Initial egg size is assumed to be 1.8 mm and anchovy growth is parameterized by the Gompertz equation of Dulcic (1997) based on measurements of *Engraulis engrasicolus* (L.) in the northern Adriatic Sea It represents average growth conditions when compared to other available data on different anchovy species (Figure 3A, grey line)

$$L_t = a \exp (be^c) \tag{2}$$

Here L_t is the length of the larvae at a given time (*t*), *a* (36.87 mm) is an asymptote representing the predicted length at metamorphosis into juveniles and *b* and *c* are constants with values 2.609 and 0.077, respectively. The Gompertz equation ensures that different growth rates of different larval stages are being captured. This is important, as small larvae (8 mm) have been shown to grow fast at a rate of 0.94 mm d^{-1}, but 14.3 mm larvae (14 day old) grew fastest at a rate of 1.06 mm d^{-1} (Dulcic, 1997). Daily growth increment decreases to a minimum of 0.43 mm d^{-1} for 31 mm larvae (36 day old) (Dulcic, 1997). Other studies reported the same trend (Palomera *et al.*, 1988; Chiu and Chen, 2001). We recall that mortality of anchovy larvae is not explicitly included in this model.

Growth in the model is temperature dependent and has been adapted from Hewett and Johnson (1992). Growth is scaled by a temperature function *f(T)* calculated using an optimal temperature T_{opt} = 25°C and a maximum temperature T_{max} = 37°C together with a Q_{10} = 2.0. The temperature coefficient Q_{10} is a measure of the rate of change of anchovy growth as a consequence of increasing the temperature by 10°C. This ensures that growth increases slowly from 0 at 0°C, reaching 1.0 at the optimal temperature of 25°C and then dropping to zero at the maximum temperature (Figure 3B). The temperature control in this case is equal to unity (i.e. optimal) at the maximum mixed layer temperature of 25°C. It becomes sub-optimal at higher temperatures because there is evidence that larval growth slows down when temperatures exceed 25°C (Chiu and Chen, 2001), which was observed in surface waters of the Black Sea during anomalously warm years such as in the late summer of 2001. Such a decrease in growth rate at high temperatures has also been used in anchovy models for other regions such as the Chesapeake Bay (Luo and Brandt, 1993; Rose *et al.*, 1999).

Results

Environmental Conditions

The larval IBM was run for the years 2001, 2002 and 2003, which offered contrasting environmental
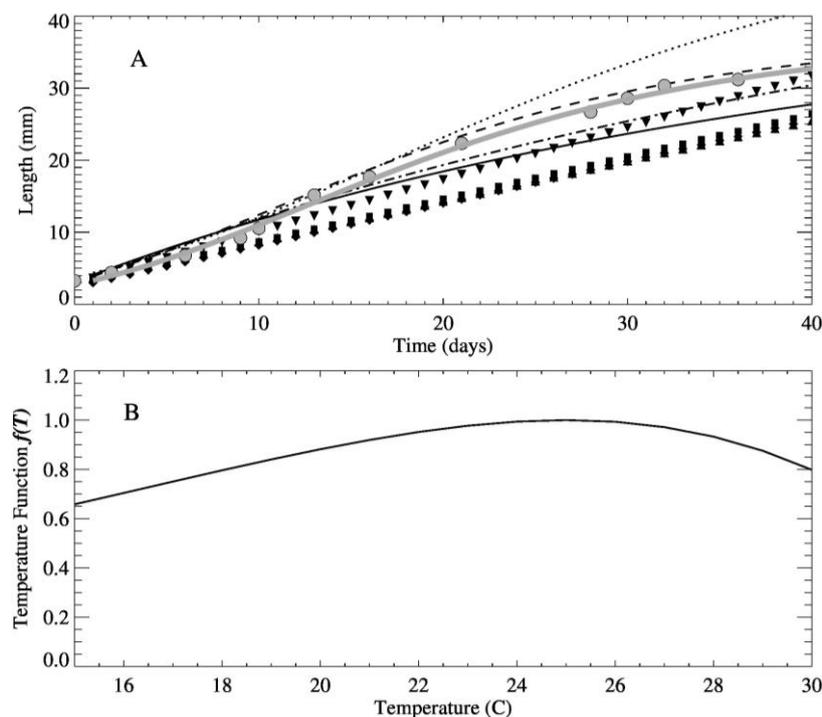
Figure 3. A) Observed length of *Engraulis encrasicolus* larvae over time. Black lines refer to observations reported by Palomera *et al.* (1988): dashed and dotted line, Chiu and Chen (2001): solid and dash-dotted line. Symbols refer to observations reported by ◆, σ: Castro and Cowen (1991), τ, ν: Rilling and Houde (1999) and λ: Dulcic (1997). Thick grey line marks the growth model reported by Dulcic (1997) that is used in this study. B) Temperature limitation function for larval growth after Hewett and Johnson (1992).
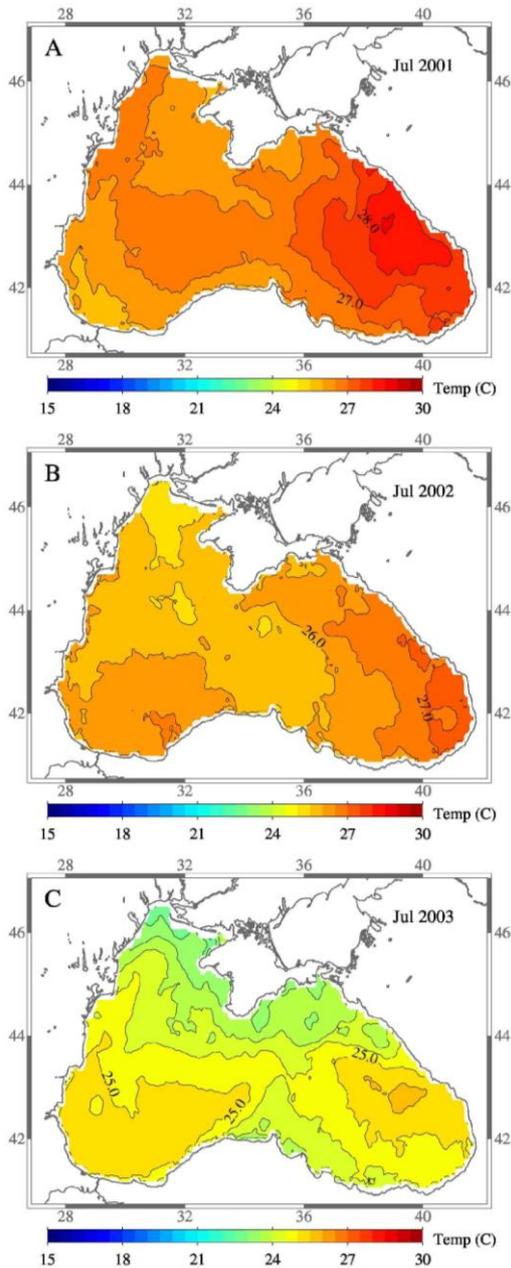
Figure 4. Monthly mean surface temperature from July15[th] to August 15th of A) 2001, B) 2002, and C) 2003 showing contrasting temperature conditions between years.
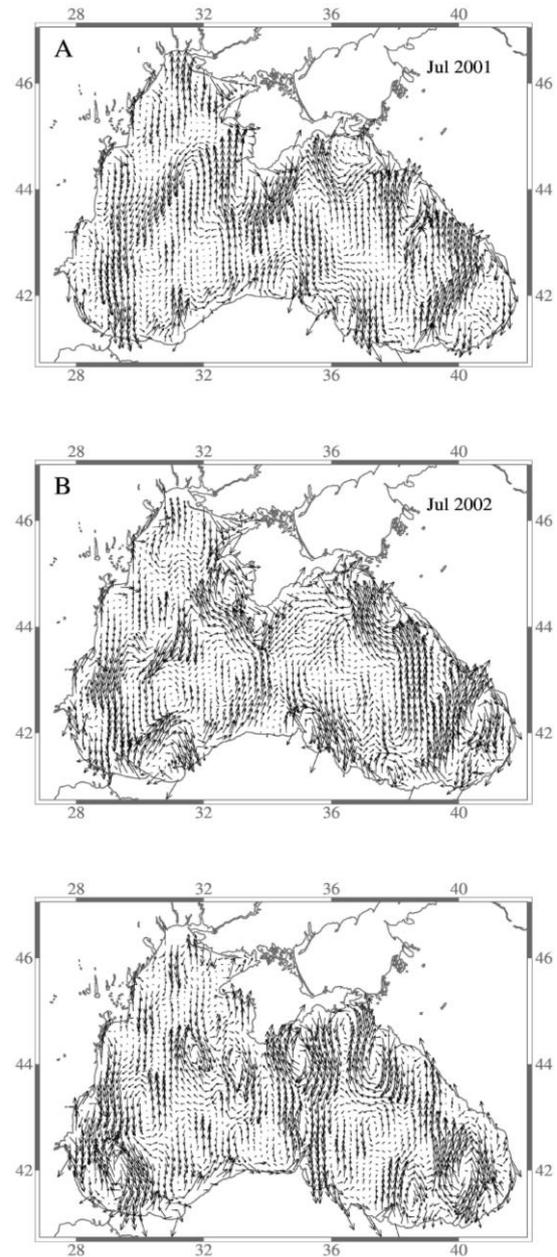
Figure 5. Monthly mean surface circulation from July 15th to August 15th of A) 2001, B) 2002, and C) 2003 showing differences in circulation patterns between years.

conditions (Figures 4, 5). 2001 was an anomalously warm year, with a very warm winter and summer season compared to other years of the 1990s and 2000s (McQuatters-Gollop *et al.*, 2008). At the beginning of June, temperatures were relatively low but then mean SSTs of 26°C in the southwest and 28°C in the east of the Black Sea developed in July/August (Figure 4A) that decreased only slightly in August/September 2001 with temperatures ranging between 24-26.5°C. The following year, 2002, was cooler with maximum SSTs in July/August between 25-27°C (Figure 4B) and 23-25.5°C in August/September. The coldest year in this study is 2003, whose SSTs were lower throughout most of the

year than the mean SSTs of the years 1997-2005 (McQuatters-Gollop *et al.*, 2008). Maximum temperatures in July/August are significantly lower than the previous years and were in the range of 23-25.5°C (Figure 4C), the spatial pattern showing two warm regions of 25°C in the west and up to 25.5°C in the eastern gyre. August/September SSTs were similar to those in 2002 (22-25.5°C) with a similar spatial pattern to the previous month, but with colder temperatures moving in from the north.

Surface circulation fields showed variations in flow conditions between different years. During July 2001 a meandering Rim Current, a wide area of southward flow south of Crimea between the eastern

and western cyclonic gyre deominated the mean circulations (Figure 5A), with very weak Batumi and anticyclonic eddies. The interior basin consisted of a series of cyclonic eddies instead of two sub-basin scale gyres. The coastal zone onshore of the Rim Current comprised of a series of anticyclonic eddies around the periphery (Figure 5a). A similar structure with some differences in the mesoscale features also persisted for the other years. In July 2002, two distinct cyclonic gyres (Eastern and Western) were present in the interior basin with a more confined southward flow from the Crimea towards the Turkish coast between the two gyres (Figure 5B). In addition, the western gyre contained two separate cyclonic gyres while the eastern gyre contained three distinct cyclonic gyres at this time. In particular, the eastern end of the basin consisted of strong currents associated with the Batumi and Caucasus anticyclonic eddies. On the other hand, in July 2003 the mean circulation map did not show the distinct pattern of the Rim Current (Figure 5C). Instead, the peripheral circulation field was dominated by small scale anticyclonic eddies, though the Batumi eddy was slightly weaker with respect to 2002. Such a mesoscale dominated flow field also existed within the interior basin, which was characterized by five smaller cyclonic gyres and strong southward flow across the basin that was located further east than in 2002.

Larval Trajectories

Model results for virtual anchovy larvae released in mid-July 2002 at four of the 15 release areas are shown in Figure 6. The information displayed in this figure is two-fold: following the dots shows the transport pathways of each drifter, while the different colors of the dots signify different developmental stages of each virtual larvae during the dispersal process. Of the virtual larvae released on the lower northwestern shelf (area 9), 46% stayed and matured in the release area, few are transported north-east to adjacent shelf regions and 22% were transported southward by the Rim Current and reached as far as the Turkish coast of the Bosporus Strait and off Sakarya River discharge zone during the 36 day simulation (Figure 6A). Transport pathways included meanders caused by the mesoscale flow field. Few virtual larvae experienced southward transport as early larva or larva stages but this mainly occurred in the late larva phase.

Particles released from the southwestern shelf off the Bosporus (area 1) were transported eastward, again following the Rim Current, and turned north following the strong northward flow of the western gyre (Figure 5B). Because this area is rather long and narrow along the coast, many of the drifters originating in the west, though drifting eastward were still in area 1 by the end of the 36-day simulation (54%). However, 37% of the drifters reach area 12 in the open Black Sea and 7% even reached the southern part of the northwestern shelf (area 11). Of those virtual anchovy leaving area 1 most had developed into early to late larva stages by that time.

Drifters released from the southern shelf off Samsun (area 3) were mainly transported northward
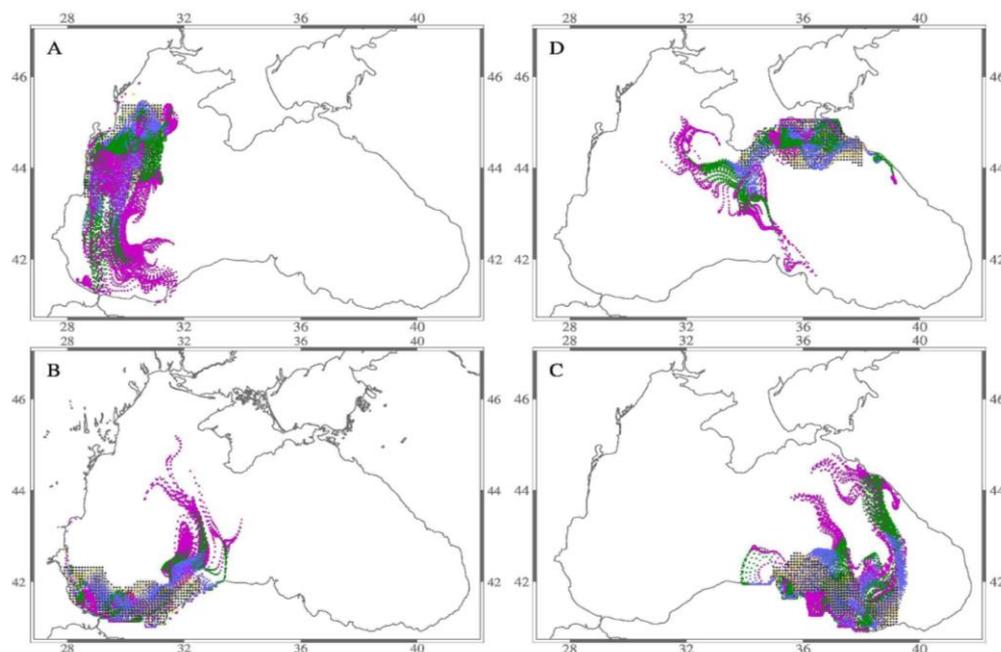
Figure 6. Trajectories of anchovy larvae released on July 15th 2002 on A) the lower northwestern shelf (area 9), B) the southwestern shelf off the Bosporus (area 1), C) the southern shelf off Samsun (area 3), and D) off Kerch Strait (area 6). Daily locations are recorded for 36 days of simulation. Larval stages are color-coded as: eggs in black, yolk sac larva orange, early larva (<10 mm) blue, larva (<20 mm) green, late larva magenta.

by two separate currents across the eastern gyre, that were created by the separation of the eastern gyre in 3 cyclonic gyres as seen in Figure 5B. 8% of the drifters were transported to area 6 near Kerch Strait and 17% to the adjacent area 5, crossing the entire Black Sea during the simulation time. Virtual larvae moving northward with the eastern current started their transport in the early larva stage and developed into late larva along the way, while those advected northward in the western current left their release area at a later time, when they had already developed into late larvae.

73% of the virtual anchovy leaving from area 6 off Kerch Strait (Figure 6D) were retained in the area, a higher percentage than those leaving from the other three regions. But the rest dispersed towards south-west along the Caucasian coast, with 11% ending up in area 5 (as most drifters followed the same pathway it is hard to differentiate between drifters). But drifters were also advected both in the westward direction (following the Rim Current), as well as towards the south (following the currents of the eastern gyre) reaching all the way to area 3 off Samsun within only 36 days. These results suggest that there is a high potential for larval dispersal after spawning.

Interannual variability of the larval transport mechanism was also examined by following virtual anchovies released from areas 6 and 9 in July of 2001 to 2003. These two regions on the north-western shelf and off Kerch Strait were chosen for a detailed analysis because they represent well-known regions of intense anchovy spawning. While most particles released on the lower northwestern shelf (area 9) followed the Rim Current towards the south (Figure 7A-7C) the influence of anticyclonic eddies near Sakarya River (Figure 7B) and off Bosporus (Figure 7C) significantly influenced late larval stage delivery locations along the southern Black Sea coast after 36 days of transport in the simulation years 2002 and 2003, respectively.

The strong variability between years was more apparent for particles released off Kerch Strait (Figure 7D-7F) where they were transported southward in a wide band across the central Black Sea in the 2001 simulation and only few particles followed the meander of the Rim Current westward. In the 2002 simulation, in contrast, most particles stayed in the area off Kerch Strait, and were entrained by the anticyclonic Caucasus eddy. A few of them followed the Rim Current eastward and were advected onto the northwestern shelf, while only 5 drifters were transported across the central Black Sea to the southern coast. In the 2003 simulation, the situation was similar to 2002 with an equal number of drifters
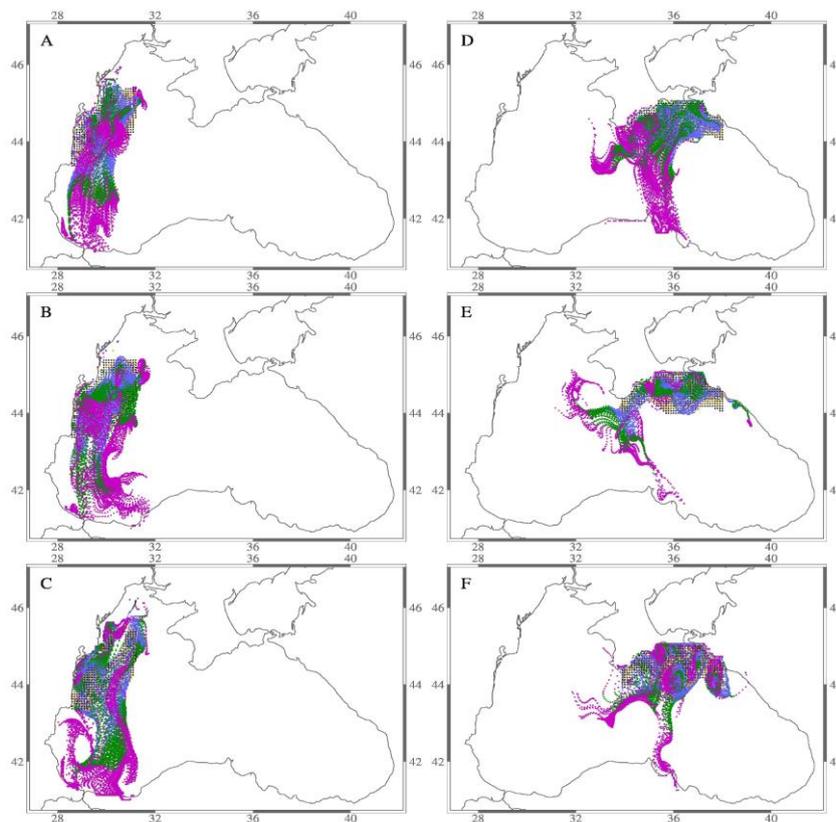
Figure 7. Trajectories of anchovy larvae released on the northwestern shelf (area 9) on 15th July A) 2001, B) 2002, and C) 2001. Trajectories of anchovy larvae released off Kerch Strait (area 6) on 15th July D) 2001, E) 2002, and F) 2003. Daily locations are recorded for 36 days of simulation. Larval stages are color-coded as: eggs in black, yolk sac larva orange, early larva (<10 mm) blue, larva (<20 mm) green, late larva magenta.

that were advected southwestward and southward. Interestingly, the drifters remaining near Kerch Strait extended much further southward into the open Black Sea in the July 2003 simulation because they were entrained in the Crimea and Caucasus eddies that extended further from the coast (Figure 5C) in comparison to July 2002 (Figure 5b). This suggests that the strong potential for larval dispersal after spawning is observed every year, however inter annual variations in larval transport pathways and delivery change in response to the variable mesoscale circulation patterns such as the coastal anticyclonic eddies (Figure 5).

While interannual variability in larval dispersal and delivery was expected, a certain degree of variability, though less than between years, was also observed between drifter simulations of different months of the same year 2002. Particles released on the lower northwestern shelf (area 9) followed the flow of the Rim Current towards the south (Figure 8a-8c) but anticyclonic coastal eddies influenced late larvae stage delivery locations along the southern Black Sea coast. This was also observed for drifters released from near Kerch Strait (area 6) where the general transport pattern of particles being transported westward and southward did not change, but the details of it did (Figure 8D-8F). Interestingly, the transport eastward towards area 5, which constitutes a

significant amount of drifters in the July and August simulations, was absent in the June simulation.

Connectivity

To summarize the role of hydrodynamic processes on the dispersal of anchovy larvae and how they vary from year to year, model results were analyzed for all 15 different release regions within the Black Sea. This was done to aggregate model results in geographic terms and help avoid too much focus on small-scale patterns that may be less reliable. Therefore, the dispersal of anchovy larvae, as displayed in Figures 7 and 8 for spawning areas on the north-western shelf and off Kerch only, was depicted as a measure of connectivity between all geographic regions. The connectivity for the July 2001-2003 simulations was calculated as the percentage of particles that left from one area (source) and were transported to another area (sink) at the end of 36-day simulations, regardless of the developmental stage reached by each particle (Figure 9). Note that releases were restricted to areas where sea surface temperatures were >20°C, hence the number of drifters (*N*) varies from simulation to simulation. Once drifters were released temperature influenced the growth rate of anchovy larvae with cooler waters slowing growth down and warmer
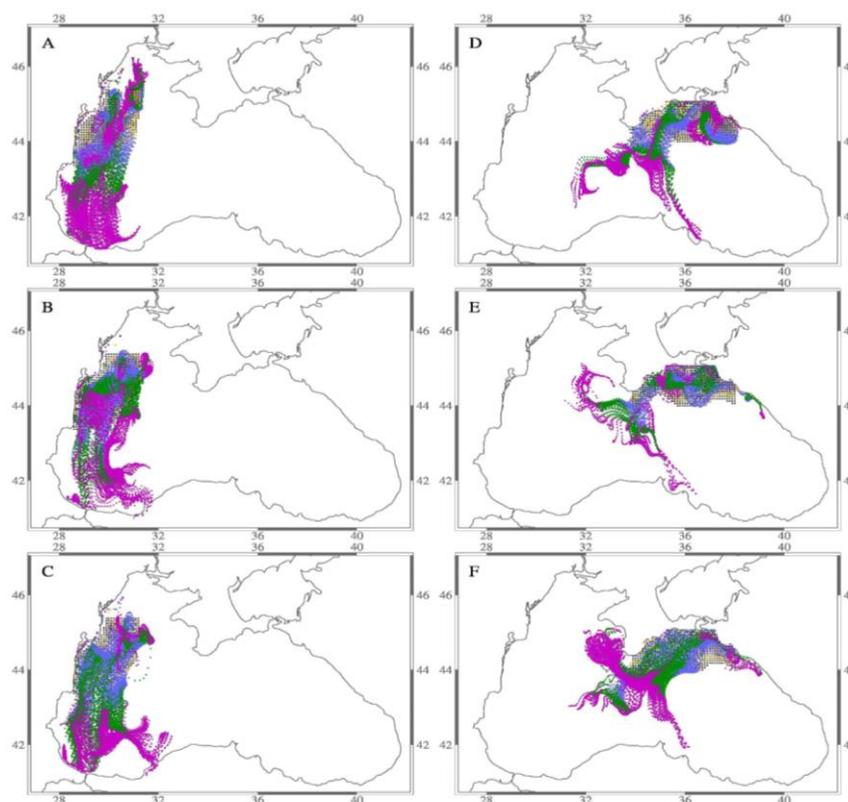
Figure 8. Trajectories of anchovy larvae released on the northwestern shelf (area 9) on A) 15th June, B) 15th July, and C) 15th August 2002. Trajectories of anchovy larvae released off Kerch Strait (area 6) on D) 15th June, E) 15th July, and F) 15th August 2002. Daily locations are recorded for 36 days of simulation. Larval stages are color-coded as: eggs in black, yolk sac larva orange, early larva (<10 mm) blue, larva (<20 mm) green, late larva magenta.
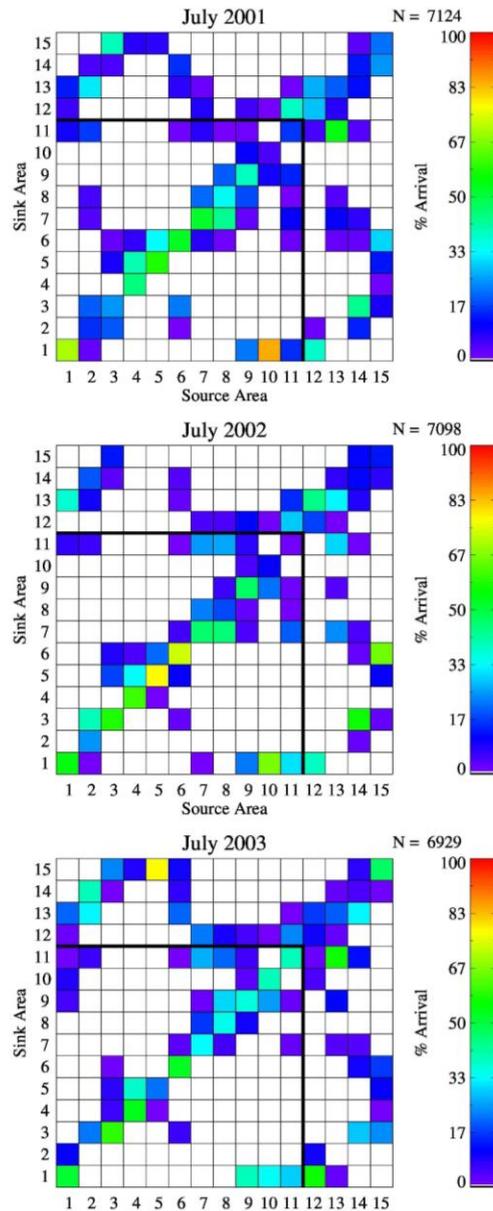
Figure 9. Connectivity matrices for modeled anchovy larvae released on the 15th of July in each of the years 2001, 2002, and 2003. Matrices indicate the probability (%) for anchovy larvae originating from a source area (x-axis) to be transported to a sink area (y-axis) estimated from individual 36-day trajectories. Thick black line separates shelf regions from open ocean regions >2000 m (areas 12-15).

environment enhancing growth (see Figure 3B). The diagonal line of the connectivity matrix represents the percentage of particles remaining within their source area, which may be interpreted as a measure of retention.

Coastal areas showed generally higher retention rates than the open ocean areas in all three simulations (Figure 9a-9c) with the exception of area 15 in the July 2003 simulation. Of the coastal regions, 1 and 4-7 had relatively high retention rates of between 30-60% in all simulations except for area 5, where it varied from 21 to 77% between years (Figure 9). Area 2 (on the southern coast) as well as area 10 (off Bulgaria) showed very low to no retention, and virtual

larvae left area 2 to be transported downstream and offshore at times (2003, Figure 9c) and towards area 1, 7 and 8, into the opposite direction at other times (2001, Figure 9A). Area 10 was connected to area 1 downstream. Open ocean regions however showed a very high rate of dispersal, mainly to the regions 3-7.

Looking at connectivity matrices it becomes apparent that the lower northwestern shelf (area 9) is well connected to the region on the southwestern shelf off the Bosphorus (area 1) with 22-40% of the virtual larvae reaching there within 36 days over the different years (Figure 9A-9C). At the same time, the area on the southern shelf off Samsun (area 3) is connected to the northeast spawning region off the Azov Sea (areas

6 and 5) with 7.5-17% of the virtual larvae reaching there (Figure 9A-9C). However, the rest of the southern coastal zone and the northwest and northeast areas are much more isolated.

Discussion

Simulation results showed for the first time the high potential for anchovy larval dispersal after spawning in the Black Sea. Often only 50% or less of the virtual larvae were retained in their release areas while the rest were transported up to 500 km across the Black Sea. Simulations showed that larvae are mainly advected by the Rim Current circulation around the periphery of the basin and the two cyclonic sub-basin gyres, and the advection is locally controlled by mesoscale eddies. Consistent with the observed circulation fields, strong meridional transport from the northern to the southern coastal zone along the western coast and the central basin exists, crossing the Black Sea in only one month. The peripheries of both the western and the eastern cyclonic gyres are also associated with large larval transports from the south coast offshore. Advection by currents is strong enough to disperse larvae over large areas. Simulations showed that the southern part of the northwestern shelf is connected to the area on the southwestern shelf off the Bosphorus Strait, while the area on the southern shelf off Samsun is connected to the northeast region off the Azov Sea. Elsewhere the connectivity between areas is not as well pronounced due to weaker and patchy current fields. Larvae traveling along these two routes encounter different temperature profiles and hence show slightly different larval growth rates. However, the effect on anchovy growth rates in this simple model is rather low. Larvae released in the northwest experience lower water temperature compared to those released in the southeast, and mature to late larvae at slightly about 0.5 days later. Interannual variability of the dispersal is considerable when comparing the warm year (2001) to cold year (2003), which is due to changes in surface currents. Growth rates are also affected by the difference in temperature from year to year, with larvae reaching juvenile stages up to 1 day earlier. Variability in dispersal is also noticeable between spawning times (June to August).

Though this study finds a high dispersal potential of anchovy larvae up to 500 km across the Black Sea in just 36 days, as well as a strong climate-induced interannual variability, these results are on similar scales to other connectivity studies that have been carried out in different seas, such as on anchovy larvae in the Benguela (Mullon *et al.*, 2003; Parada *et al.*, 2003) and Peru regions (Xu *et al.*, 2013), benthic larvae in the Caribbean Sea (Cowan *et al.*, 2006), Antarctic krill larvae in the Scotia Sea (Fach and Klinck, 2006; Fach *et al.*, 2006), as well as Lobster larvae in the Gulf of Maine (Xue *et al.*, 2008; Incze *et al.*, 2010). For example, it has been shown that in the southern Benguela important spawning grounds of anchovy may be hundreds of kilometers away from nursery areas (Parada *et al.*, 2003), while for different reef fishes in the Caribbean, typical dispersal distances were on the order of tens to hundreds of kilometers (Cowen *et al.*, 2006). In addition, it was shown that the Antarctic krill population at South Georgia in the Southern Ocean is supplied by larvae originating more than 1500km upstream along the Antarctic Peninsula (Fach and Klinck, 2006; Fach *et al.*, 2006).

For the design of a network of MPA's in the Black Sea it is of importance that this study for the first time showed clearly the strong connectivity between regions far apart. Particularly the southern part of north-western shelf (area 9) is connected to the region on the southwestern shelf off the Bosphorus (area 1) as well as the southern shelf off Samsun (area 3) is connected to the northeast Black Sea off the Azov Sea (areas 6 and 5) via ocean currents when assuming a 36-day pelagic larval duration. Design of MPA's should therefore focus on these regions, although it should be noted, that this study is based on anchovy larvae and that species with different pelagic larval durations will show different connectivity patterns (Rossi *et al.*, 2014).

While this study is only a first step towards analyzing the complex topic of anchovy larval dispersal in the Black Sea, it has demonstrated the strong hydrodynamic influence on the distribution of early anchovy life stages. These results suggest that it may be an over-simplification to assume that anchovy movement across the Black Sea occurs only via active overwintering and/or spawning migration as generally accepted (Ivanov and Beverton, 1985; Chashchin, 1996). However, the use of geostrophic currents in this study may not be entirely satisfactory to represent ocean currents and sub-grid scale turbulent dispersion realistically. One immediate next step would be running the larval IBM embedded in a high resolution ocean circulation model to account for a more realistic representation of the flow field as well as to enable the possibility of including vertical displacement of anchovy through currents as an additional mechanism that may influence dispersal. Another step may be to extend the IBM to include more sophisticated bioenergetics equations that already exist (Oguz *et al.*, 2008) to test for the influence of food availability on anchovy survival during transport The present model stops at the juvenile stage, but could be extended to include active movement during search for food or behavioral swimming of older anchovy stages. These extensions may assist in understanding how anchovy distribution is determined and how it might change in the future with anticipated climatic changes in the Black Sea environment.

By itself or used in complement with otolith chemistry (Ashford *et al.*, 2010) or genetic studies on anchovy (Karahan and Ergene, 2011), the technique

used in this study is an innovative approach to resolve planktonic early life stage dispersal and connectivity of marine populations related to the physical circulation of different oceanic systems.

Acknowledgements

References

Ashford, J.R., La Mesa, M., Fach, B.A., Jones, C. and Everson, I. 2010. Testing early life connectivity using otolith chemistry and particle-tracking simulations. Canadian Journal of Fisheries and Aquatic Sciences, 67: 1303-1315.

Chashchin, A.K. 1996. The Black Sea populations of anchovy. Scientia Marina, 60(2): 219-225.

Chiu, T.S. and Chen, C.S. 2001. Growth and temporal variation of two Japanese anchovy cohorts during their recruitment to the East China Sea. Fisheries Research, 53(1): 1–15. doi:10.1016/S0165-7836(00)00294-0.

Cowen, R.K. and Sponaugle, S. 2009. Larval dispersal and ma- rine population connectivity, Annu. Rev. Mar. Sci., 1: 433– 466.

Cowen, R.K., Paris, C.B. and Srinivasan, A. 2006. Scaling of connectivity in marine populations, Science, 311: 522-527. doi: 10.1126/science.1122039

Dulcic, J. 1997. Growth of anchovy *Engraulis encrasicolus* (L.), larvae in the North Adriatic Sea. Fisheries Research, 31: 189-195.

Einarsson, H. and Gürtürk, N. 1960. Abundance and distribution of eggs and larvae of anchovy (*Engraulis encrasicolus ponticus*) in the Black Sea. Publications of the Hydrobiological Research Institute, Faculty of Sciences, University of Istanbul: 71-94.

Fach, B.A. and Klinck, J.M. 2006. Transport of Antarctic krill (*Euphausia superba*) across the Scotia Sea. Circulation and Particle Tracking Simulations. Deep-Sea Research, 53(1): 987-1010.

Fach, B.A., Hofmann, E.E. and Murphy, E.J. 2006. Simulations of circulation dynamics in the Scotia Sea and their implication on the transport of Antarctic krill. Krill survival. Deep-Sea Research, 53(6):1011-1043.

Game, E.T., Grantham, H.S., Hobday, A.J., Pressey, R.L., Lombard, A.T., Beckley, L.E., and Richardson, A.J. 2009. Pelagic protected areas: the missing dimension in ocean conservation. Trends in ecology & evolution, 24(7): 360-369.

Garcia, A. and Palomera, I. 1996. Anchovy early life history and its relation to its surrounding environment in the Western Mediterranean basin. Scientia Marina., 60(2): 155-166.

Hewett, S.W. and Johnson, B.L. 1992. Fish bioenergetics model 2. University of Wisconsin Sea Grant Technical Report No. WIS-SG-92-250.

Incze, L., Xue, H., Wolff, N., Xu, D., Wilson, C., Steneck, R., Wahle, R., Lawton, P., Pettigrew, N. and Chen, Y. 2010. Connectivity of lobster (*Homarus americanus*) populations in the coastal Gulf of Maine: Coupled Biophysical Dynamics. Fisheries Oceanography, 19(1): 1–20. doi:10.1111/j.1365-2419. 2009.00522.x

Ivanov, L. and Beverton, R.J.H. 1985. The fishery resources of the Mediterranean. Part two: Black Sea. G.F.C.M. Studies and Reviews. 60, FAO: Rome, 135pp.

Karahan, A. and Ergene, S. 2011. Chromosomal differentiation between populations of *Clarias gariepinus* (Burchell, 1822) from the Goksu Delta and Orontes River (Turkey). Turkish Journal of Biology 35(1):79-87.

Kideys, A.E., Gordina, A.D., Bingel, F. and Niermann, U. 1999. The effect of environmental conditions on the distribution of eggs and larvae of anchovy (*Engraulis encrasicolus L.)* in the Black Sea. ICES Journal of Marine Science, 56: 58-64.

Korotaev, G., Oguz, T. Nikiforov, A. and Koblinsky, C. 2003. Seasonal, interannual, and mesoscale variability of the Black Sea upper layer circulation derived from altimeter data, Journal of Geophysical Research, 108(C4), 3122, doi:10.1029/2002JC001508.

Lester, S., Halpern, B., Grorud-Colvert, K., Lubchenco, J., Ruttenberg, B., Gaines, S., Airamé, e, S. and Warner, R.R. 2009. Biological effects within no take marine reserves: a global synthesis, Mar. Ecol. Prog. Ser., 384: 33–46.

Lisovenko, L.A. and Andrianov, D.P. 1996. Reproductive biology of anchovy (*Engraulis encrasicolus ponticus Alexandrov 1927*) in the Black Sea. Scienta Marina, 60(2): 209-218.

Luo, J. and Brandt, S.B. 1993. Bay anchovy *Anchoa mitchilli* production and consumption in mid-Chesapeake Bay based on a bioenergetics model and acoustic measures of fish abundance. Marine Ecology Progress Series, 98: 223-236.

McQuatters-Gollop A., Mee, L.D., Raitsos, D.E. and Shapiro, G.I. 2008. Non-linearities, regime shifts and recovery: The recent influence of climate on Black Sea chlorophyll. Journal of Marine Systems, 74: 649-658. doi:10.1016/j.jmarsys.2008.06.002

Moffitt, E.A., Botsford, L.W., Kaplan, D.M. and O'Farrell, M.R. 2009. Marine reserve networks for species that move within a home range. Ecological Applications, 19: 1835–1847.

Moffitt, E.A., White, J.W. and Botsford, L.W. 2011. The utility and limitations of size and spacing guidelines for designing Marine Protected Area networks, Biol. Conserv., 144: 306–318.

Mullon, C., Fréon, P., Van Der Lingen, C. and Huggett, J. 2003. From particles to individuals: modelling the early stages of anchovy (*Engraulis capensis/ encrasicolus*) in the southern Benguela. Fisheries Oceanography, 12(4/5): 396–406. doi: 10.1046/j.1365-2419.2003. 00240.x.

Niermann, U., Bingel, F., Gorban, A., Gordina, A.D., Gücü, A.C., Kideys, A.E., Konsulova, A., Radu, G., Subbotin, A.A. and Zaika, V.E. 1994. Distribution of anchovy eggs and larvae (*Engraulis encrasicolus* Cuv.) in the Black Sea in 1991-1992. ICES Journal of Marine Science, 51: 395-406.

North, E.W. and Houde, E.D. 2004. Distribution and transport of bay anchovy (*Anchoa mitchilli*) eggs and larvae in Chesapeake Bay. Estuarine, Coastal and Shelf Science, 60: 409-429.

Oguz, T. and Besiktepe, S. 1999. Observations on the Rim Current structure, CIW formation and transport in the western Black Sea, Deep Sea Research, 46: 1733–

1753.

Oguz, T., Ashwini, D. and Malanotte-Rizzoli, P. 2002. On the role of mesoscale processes controlling biological variability in the Black Sea: Inferences from SeaWiFS-derived surface chlorophyll field, Continental Shelf Research, 22: 1477–492.

Oguz, T., Salihoglu, B. and Fach, B.A. 2008. A coupled plankton-anchovy population dynamics model assessing nonlinear controls of anchovy and gelatinous biomass in the Black Sea. Marine Ecology Progress Series, 369: 229-256.

Oguz, T., Tugrul, S., Kideys, A.E., Ediger, V. and Kubilay N. 2005. Physical and biogeochemical characteristics of the Black Sea. In: A.R. Robinson and K.H. Bring (Eds.), The Sea, Harvard University Press, Cambridge, 14(33): 1331-1369.

Palomera, I., B. Morales-Nin, B. and Lleonart, J. 1988. Larval growth of anchovy, Engraulis encrasicolus, in the Western Mediterranean Sea. Marine Biology, 99: 283-291.

Parada, C., Van Der Lingen, C.D., Mullon, C. and Penven, P. 2003. Modelling the effect of buoyancy on the transport of anchovy (*Engraulis capensis*) eggs from spawning to nursery grounds in the southern Benguela: an IBM approach Fisheries Oceanography, 12(3): 170–184.
    doi: 10.1046/j.1365-2419.2003.00235.x

Pelc, R.A., Warner, R.R., Gaines, S.D. and Paris, C.B. 2010. Detecting larval export from marine reserves. Proc Natl Acad Sci, USA, 107: 18266−18271

Rose, K.A., Cowan, J.H., Clark, M.E., Houde, E.D. and Wang, S.B. 1999. An individual-based model of bay anchovy population dynamics in the mesohaline region of Chesapeake Bay. Marine Ecology Progress Series, 185: 113-132.

Rossi, V., Ser-Giacomi, E., López, C., and Hernández-García, E. 2014. Hydrodynamic provinces and oceanic connectivity from a transport network help designing marine reserves, Geophys. Res. Lett., 41: 2883–2891, doi:10.1002/2014GL059540.

Satilmis, H.H., Gordina, A.D., Bat, L., Bircan, R., Culha, M., Akbulut, M. and Kideys, A.E. 2003. Seasonal distribution of fish eggs and larvae off Sinop (the southern Black Sea) in 1999-2000. Acta Oecologica, 24: 275-280

Sorokin, Y.I. 2002. The Black Sea ecology and oceanography. Backhuys Publishers, Leiden, 875 pp.

Treml, E., Roberts, J., Chao, Y., Halpin, P.N., Possingham, H. and Riginos, C. 2012. Reproductive output and duration of the pelagic larval stage determine seascape-wide connectivity of marine populations, Integr. Comp. Biol., 52(4): 525–537.

Xu, Y., Chai, F., Rose, K.A., Niquen, C.M. and Chavez, F.P. 2013. Environmental influences on the interannual variation and spatial distribution of Peruvian anchovy (*Engraulis ringens*) population dynamics from 1991 to 2007: A three-dimensional modeling study. Ecological Modeling, 264: 64-82.
    doi:10.1016/j.ecolmodel.2013.01.009

Xue, H., Incze, L., Xu, D., Wolff, N. and Pettigrew, N. 2008. Connectivity of lobster populations in the coastal Gulf of Maine: Circulation and larval transport potential. Ecological Modelling, 210(1–2): 193–211.
    doi:10.1016/j.ecolmodel.2007.07.024